Spent Fuel Heating Analysis Code for Consolidated and Unconsolidated Fuel*

L.E. Fischer

Lawrence Livermore National Laboratory, Livermore, California, United States of America

INTRODUCTION

Many nuclear power plants are running out of storage space in their reactor pools for storing spent fuel. On-site Independent Spent Fuel Storage Installations (ISFSIs) can be used to store excess spent fuel. All ISFSIs, both wet and dry types, must be licensed under 10 CFR 72. To license an ISFSI, a utility must submit a Safety Analysis Report (SAR) to demonstrate that the ISFSI design, construction, and operation comply with the requirements of 10 CFR 72. For cask storage systems, the SAR may reference a Topical Safety Analysis Report (TSAR) which has been submitted by a cask supplier and shows compliance with 10 CFR 72.

One of the requirements that must be evaluated in a TSAR or SAR is contained in 10 CFR 72.73(h) which states that the fuel cladding shall be protected against degradation and gross rupture. The primary approach currently used to demonstrate compliance with 10 CFR 72.73(h) is to limit the fuel cladding temperature to a maximum value and to demonstrate that the maximum temperature value is not exceeded during storage operations. Several methods, including computer codes, have been developed or are being developed for calculating the maximum temperatures of fuel rods in spent fuel bundles.(Wooton 1983, Cox 1977, Rector 1986, McCann 1986, Fischer 1985) The validity and complexity of any method is usually dependent on the assumptions used in modeling the rod configuration for the three modes of heat transfer: radiation, conduction, and convection.

One calculational method used extensively in licensing casks for transporting spent fuel is the Wooton-Epstein Correlation (WEC), which was developed at the Battelle Memorial Institute in 1963 (Wooton, et al., 1987). The WEC is based on a simplified radiative heat transfer model, which replaces the fuel rod rows with equivalent concentric tubes. This paper describes the development and benchmarking of the Spent Fuel Rod Heating Analysis (SFHA) computer code, which is based on the use of concentric tube models for radiative and conductive heat transfer. SFHA is compiled in Basic for use on IBM-compatible personal computers. It is used at LLNL in the evaluation of TSAR and SAR submittals to check their compliance with 10 CFR 72.73(h).

SYMBOLS

The symbols used in this report are the same as those used in Ref. 1 except for changes or additions made for clarification and inclusion of conductive heat transfer.

* This work was supported by the United States Nuclear Regulatory Commission under a Memorandum of Understanding with the United States Department of Energy.

A_m = Heat transfer area (ft^2)
A_1 = Area of fuel bundle envelope (ft^2)
C_1 = Geometric constant (radiation)
C_2 = Empirical dimensional constant (free convection)
C_c = Empirical convection coefficient
F_1 = Empirical constant (radiative)
I = Ith tube or fuel rod row
K_g = Thermal conductivity coefficient for fill gas (Btu/hr ft^2 °F)
K_r = Overall thermal conductivity of fuel rod (Btu/hr ft^2 °F)
Gr_d = Grashof number
N = Number of rods in the outer row of one side of bundle
P = Fuel rod pitch (ft)
Pr = Prandtl number
Q = Q_{10} = Heating rate of bundle
T_E = Maximum fuel cladding temperature (°R)
T_c = Cask wall temperature (°R)
U = Overall conductance coefficient (Btu/hr ft^2 °F)
d = Fuel rod diameter (ft)
m = Row number beginning at outer row
n = m - 1
ε = Surface emissivity
σ = Stefan-Boltzmann constant (Btu/hr ft^2 $°R^4$)
s = Empirical exponent coefficient (convection)
h_c = Convective heat transfer coefficient (Btu/hr ft^2 °F)
t = Rod cladding thickness (ft)

HEAT TRANSFER MODES AND ANALYSIS

R. Wooton and H. Epstein performed their investigations with a simulated 17 x 17 PWR bundle in the horizontal position. The tests were performed in atmospheric air and resulted in the following correlation for radiative and convective heat transfer.

$$Q = \sigma C_1 F_1 A_1 [T_E^4 - T_c^4] + C_2 A_1 [T_E - T_c]^{4/3} . \quad (1)$$

The determinations of the constants C_1, F_1, and C_2 are discussed in Ref. 1. Wooton and Epstein thought that their correlation, Eq. (1), might be valid for other fuel assembly geometries through the use of appropriate constants, but did not have sufficient data to support their contention. Research conducted at LLNL expanded the Wooton and Epstein correlation to include other fuel assembly geometries and a heat conduction term for analyzing, in particular, consolidated fuel bundles. Heat transfer Eq. (1) was expanded to include all three modes of heat transferring, by radiation, conduction, and convection, as follows:

$$Q = \sigma C_1 F_1 A_1 [T_E{}^4 - T_c{}^4] + U\, A_1\, [T_E - T_c] + C_2 A_1 [T_E - T_c]^S , \quad (2)$$

where the constants s, C_1, C_2, and U can be determined for different gases and fuel rod configurations. Each mode of heat transfer was modeled separately and then incorporated into SFHA. SFHA benchmark calculations were then made for comparison to test data to validate the use of a simple one-dimensional heat transfer model for estimating fuel rod temperatures.

Radiative Heat Transfer

Radiative heat transfer within a bundle is calculated using concentric tube models. For square arrays of spent fuel rods the configuration factors C_1 and F_1 derived and benchmarked (Wooton 1983) are used in Eq. (2). For hexagon arrays the configuration factors derived and benchmarked (Fischer 1985) are used.

Convective Heat Transfer

The natural convective heat transfer coefficient for a single cylinder is in general calculated from Eq. (3).

$$h_c = \frac{C_c K_g}{d} [Gr_d \, Pr]^s \tag{3}$$

When benchmark calculations were performed it was found that for fuel bundles with heat fluxes in the 100-300 Btu/hr ft^2 range (typical for spent fuel storage), the flow is not turbulent in the bundle. Good correlation between test data and analysis was obtained neglecting convection, which is reasonable because the Grashof number is less than 2000 for the specified conditions. However, to cover the complete range of natural convection the heat transfer coefficient in generalized form is

$$h_c = C_2[T_E - T_c]^s, \tag{4}$$

where C_2 and s are empirically derived from test data and can be zero.

Conductive Heat Transfer

Conductive heat transfer within the bundle is handled in one dimension by using concentric tubes to represent the rod arrays. The square bundle in Fig. 1 has 49 rods and can be modeled as four equivalent concentric square tubes. The first or outer tube has seven fuel rods on each of the four sides, the second tube has five on a side, and so on until the fourth tube has only one rod. The conductive heat transfer between any two adjacent concentric tubes is calculated from the relation

$$Q_{mn} = U\, A_m \,(T_m - T_n), \tag{5}$$

where U is the overall conductance between the two tubes. From the same method used for radiative heat transfer, the temperature of the Ith tube becomes

$$\sum_{m=1}^{I} (T_m - T_n) = \frac{Q_{10} C_m}{U\, A_1}, \tag{6}$$

where C is the radiative geometric constant, which depends on a specific fuel bundle geometry. The overall conductance U also depends on a specific fuel bundle, geometry. The overall conductance is derived (Fischer 1989) for square and hexagon arrays.

For square fuel rod arrays the overall conductance is:

$$U = \left(\frac{d}{P}\right) \frac{K_g}{(P-d) + 0.215d + \frac{\pi}{4}\left(\frac{d^2}{t}\right)\left(\frac{K_g}{K_r}\right)}. \tag{7}$$

For a hexagon array the overall conductance is:

$$U = \frac{d}{P} \frac{K_g}{(P-d) + 0.08d + \frac{\pi}{4}\left(\frac{d^2}{t}\right)\frac{K_g}{K_r}}. \tag{8}$$

SFHA CODE

A computer code was written in Basic for IBM-compatible personal computers to calculate fuel rod temperatures for hexagon and square fuel bundles. For square bundles in a vacuum, the fuel rod temperature is calculated from

$$\sum_{m=1}^{I} (T_m^4 - T_n^4) = \frac{Q_{10}}{\sigma F_1 A_1} \sum_{m=1}^{I} \frac{N-(2m-2)}{N}. \tag{9}$$

For hexagon bundles in a vacuum, the fuel rod temperature is calculated from

$$\sum_{m=1}^{I} (T_m^4 - T_n^4) = \frac{Q_{10}}{\sigma F_1 A_1} \left[\frac{N}{3N(N-1)+1}\right] \sum_{m=1}^{I} \frac{3(N-m+1)(N-m)+1}{(N-m+1)}. \tag{10}$$

When air or helium is present, the fuel rod temperature is initially calculated for vacuum conditions using either Eq. (9) or (10). The resultant heat flow is then calculated using Eq. (2) and the appropriate C_1, F_1, C_2, and U_1 values and compared to the specified heat flow. If the difference between the resultant and specified heat flow normalized to the specified heat flow is greater than 0.1 percent, a revised rod temperature is calculated as the initial temperature times one minus 1 percent of the absolute heat flow difference divided by the specified heat flow. This process of revising the fuel rod temperature is repeated until the resultant heat flow converges to within 0.1 percent of the specified heat flow. The computer code assumes that the basket and fuel rod emissivities are identical.

Input data to SHFA is menu-driven by a series of questions on the screen. After all of the required information is input, the program automatically executes.

BENCHMARK RESULTS

Experimental data for five tests of a hexagon array of 217 simulated fuel rods in a vacuum environment are reported in Ref. 2. Using the computer code for a hexagon array, the fuel rod temperatures for each test condition and fuel rod row were calculated. As seen in Table 1 for the first test, the calculated and measured results for each fuel rod row agree quite well with each other for a cladding emissivity equal to 0.55, which is typical for stainless steel for the described coloration and temperature conditions. The agreement between the calculated and measured results begins to diverge at the three outer rows, as might be expected for this simple model which replaces the rods with equivalent tubes and treats a two-dimensional array as a one-dimensional model.

The calculated and measured results for the other four experiments in Ref. 2 under vacuum conditions were also in good agreement. In Table 2, the temperature results for the central rod are summarized for the five experiments. Agreement between the temperature results was improved for the last two experiments, which used a different test assembly when the assumed emissivity was 0.6.

Testing has been performed for benchmarking the COBRA and HYDRA computer codes for spent fuel storage application (Bates 1986, Cuta 1986). In Table 3 the center rod temperatures measured for an unconsolidated 15 x 15 PWR bundle as reported by Bates 1986, are compared with those calculated using SFHA. For the specified power ranges, configuration, and fill gases, the comparison between the test data and SFHA results are reasonable good and within experimental error. In all cases the thermal convection coefficient was zero.

Table 4 summarizes the center fuel rod temperatures for tests reported by Cuta 1986, for comparison with SFHA calculated results. The test sections simulated an unconsolidated 8 x 8 BWR fuel bundle for tests U1–U6, and a 126-rod consolidated BWR canister for tests 12-18. The consolidated bundle was modeled as a 7-rod hexagon fuel bundle with a 0.010-inch rod pitch gap. The comparison is good for the stated test conditions. Better agreement for the consolidated fuel might be obtained if the electrical heater rod model included the gas gap and ceramic insulator in a parallel conduction path with the rod cladding.

CONCLUSIONS

The benchmark results show that SFHA can be used to calculate spent fuel rod temperatures for square and hexagon fuel bundles under various environments for the consolidated or unconsolidated condition. When convective heat transfer is used in SFHA, the convective heat transfer coefficient and exponent must be empirically established from test data. Although SFHA is limited to analyzing symmetrical geometries and temperature distributions, it has been useful at the Lawrence Livermore National Laboratory in performing sensitivity studies and evaluating SAR submittals for a variety of spent fuel configurations and conditions.

REFERENCES

Wooton, R., Epstein, H., Bucholz, J. A., *Scoping Design Analysis for Optimizing Shipping Casks Containing 1, 2, 3, 5, 7, or 10 Year Old PWR Spent Fuel*, ORNL/CSD/TM-149 (1983), Appendix J only.

Cox, R. L., *Radiative Heat Transfer in Arrays of Parallel Cylinders*, ORNL-5329 (1977).

Rector, D. R., Wheeler, C. L., Lombardo, N. J., *COBRA-SFS: A Thermal-Hydraulic Analysis Computer Code*, PNL-6049, Vol. I-III (1986).

McCann, R. A., Lowery, P. S., *HYDRA-II: A Hydrothermal Analysis Computer Code*, PNL-6206, Vol. I-III (1987).

Fischer, L. E., *Spent Fuel Pin Temperature PC Code*, UCRL-91019 (1985).

Fischer, L. E., *Spent Fuel Heating Analysis (SFHA) Code*, UCID-21711 (1989).

Bates, J. M., *Single PWR Spent Fuel Assembly Heat Transfer Data for Computer Code Evaluations*, PNL-5571 (1986).

Cuta, J.M., Creer, J. M., *Comparisons of COBRA-SFS Calculations with Data from Simulated Sections of Unconsolidated and Consolidated BWR Spent Fuel*, EPRI NP-4593 (1986).

Table 1. Fuel rod temperature comparison test data (Run No. 1) from Ref. 2 assuming ε = 055 for a vacuum.

Row No.	Rod No.	Measured Temperature °K	Calculated Temperature °K
1	209	568	564
1	185	572	564
1	170	578	564
1	196	588	564
2	155	601	606
2	147	617	606
3	97	635	636
3	126	643	636
4	71	656	658
5	57	672	675
6	31	684	686
9	1	700	699

Table 2. Fuel rod temperature comparison test data from Ref. 2 for a vacuum.

Run No.	PDR	Measured Temperature °K	Assumed ε	Calculated Temperature °K
1	1.36	700	0.55	699
2	1.36	812	0.55	811
3	1.36	702	0.55	709
4	1.24	703	0.60	716
5	1.24	810	0.60	812

Table 3. Fuel rod temperature comparison test data from Ref. 7, assuming ε = .60.

Test No.	Fill Gas	Power Btu/hr ft^2	TEMPERATURES, °F Tube Test	Center Test	SFHA
R-7	Air	139	388	453	458
R-8	Vac	139	398	468	488
R-9	He	142	378	418	414
R-10	He	273	409	483	475
R-11	Vac	270	437	562	579
R-12	Air	267	415	532	533

Table 4. Fuel rod temperature comparison test data from Ref. 8, assuming ε = 0.8.

Test No.	Fill Gas	Power Btu/hr ft^2	TEMPERATURES, °F Tube Test	Center Test	SFHA
U1	Air	114	355	393	397
U2	Air	114	403	433	440
U3	Air	228	358	448	437
U4	Vac	114	329	381	386
U5	Vac	228	376	468	466
U6	Air	114	312	359	358
12	Air	114	385	410	418
14	Air	228	378	430	443
16	He	114	387	396	403
18	He	228	380	398	411

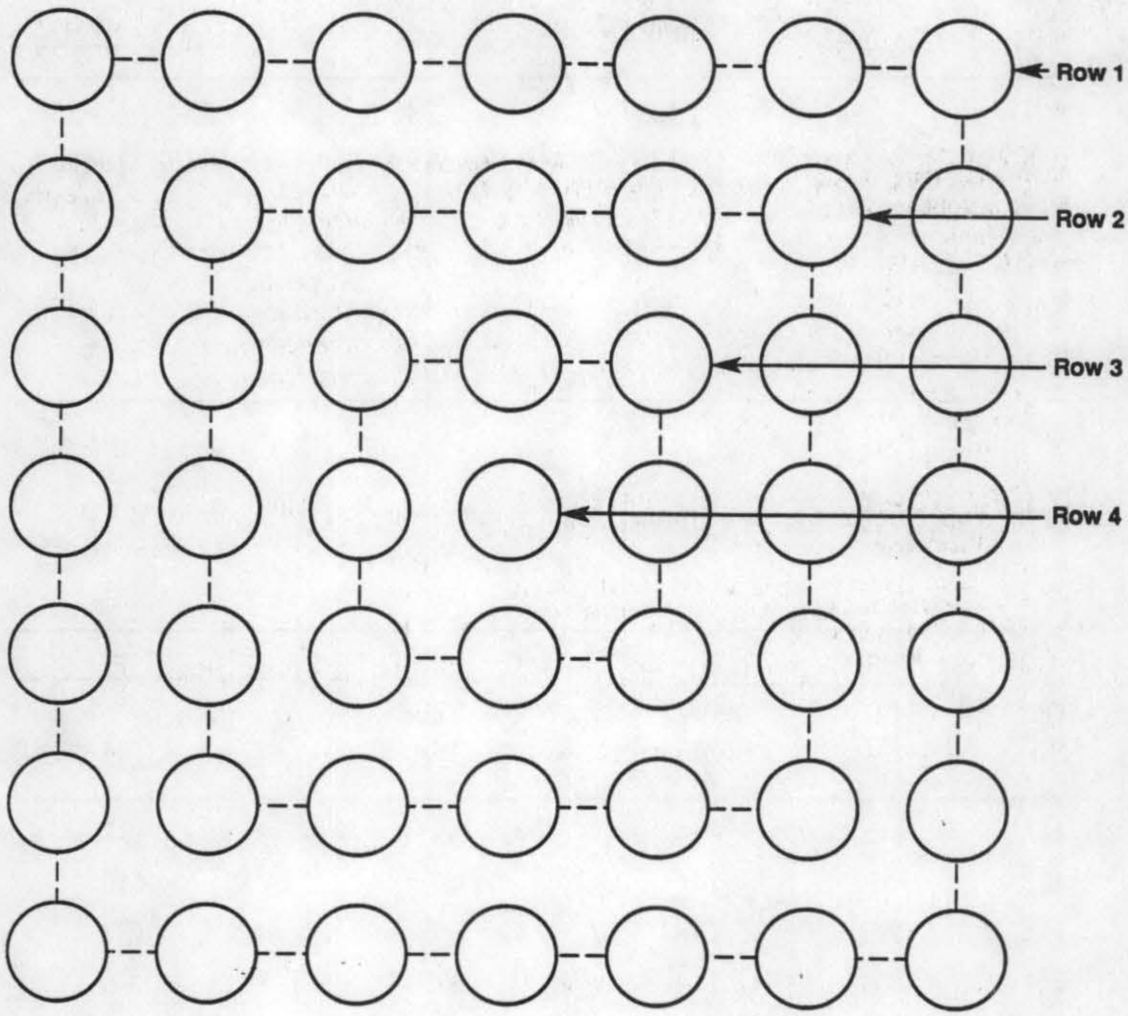

Figure 1. Numbering of rod rows for square array.